Synthesis of Optimum Process Flowsheets," Ph.D. Thesis, Univ. Florida (1974).
Stephanopoulos, G., "Synthesis of Networks of Heat Exchangers—A Self-Study Block Module," Project PROCEED, Massachusetts Institute of Technology, Cambridge, MA (1977).
Stephanopoulos, G., and A. W. Westerberg, "Overcoming Deficiencies of the Two-Level Method of Systems Optimization," *AIChE J.*, **19**, 1269 (1973).
Stephanopoulos, G., and A. W. Westerberg, "Synthesis of Optimal Process Flowsheets by an Infeasible Decomposition Technique in the Presence of Functional Non-Convexities," *Can. J. Chem. Eng.*, **53**, 551 (1975).
Stephanopoulos, G., and A. W. Westerberg, "Studies in Process Synthesis—II. Evolutionary Synthesis of Optimal Process Flowsheets," *Chem. Eng. Sci.*, **31**, 195 (1976).
Steward, D. V., "On an Approach to Techniques for the Analysis of the Structure of Large Systems of Equations," *SIAM Review*, **4**, 321 (1962).
Stupin, W. J. and F. J. Lockhart, "Thermally Coupled Distillation—A Case History," *Chem. Eng. Prog.*, **68** (10), 71 (1972).
Takamatsu, T., Y. Naka, S. Tomita and H. Ochi, "Determination of Process Structures of Azeotropic Distillation System," International Congress on Contribution of Computers. . . . , Paris, France.
Tedder, D. W., and D. F. Rudd, "Parametric Studies in Industrial Distillation, Part I. Design Comparisons," *AIChE J.*, **24**, 303 (1978a).
Tedder, D. W., and D. F. Rudd, "Parametric Studies in Industrial Distillation, Part II. Heuristic Optimization," *AIChE J.*, **24**, 316 (1978b).
Thompson, R. W., and C. J. King, "Synthesis of Separation Schemes," Technical Report No. LBL-614, Lawrence Berkeley Laboratory (1972a).
Thompson, R. W., and C. J. King, "Systematic Synthesis of Separation Schemes," *AIChE J.*, **18**, 941 (1972b).
Ugi, I., and P. Gillespie, "Chemistry and Logical Structure. 3. Representation of Chemical Systems and Interconversions by BE Matrices and their Transformation Properties," *Angew. Chem. Int. Ed. Engl.*, **10**, 914, 915 (1971).
Ugi, I., P. Gillespie and C. Gillespie, "Chemistry and Logical Structure. 6. Chemistry, A Finite Metric Topology. Synthetic Planning, an Exercise in Algebra," *Trans. N.Y. Acad. Sci.*, **34**, 416 (1972).
Umeda, T., T. Harada and K. Shiroko, "A Thermodynamic Approach to the Synthesis of Heat Integration Systems in Chemical Processes," Proc. 12th Symposium on Computer Applications in Chemical Engineering, p. 487, Montreux, Switzerland (1979).
Umeda, T., A. Hirai and A. Ichikawa, "Synthesis of Optimal Processing System by an Integrated Approach," *Chem. Eng. Sci.*, **27**, 795 (1972).
Umeda, T. and A. Ichikawa, "Synthesis of Optimal Processing Systems by a Method of Decomposition," AIChE Meeting, Dallas, TX (1972).
Umeda, T., J. Itoh and K. Shiroko, "Heat Exchange System Synthesis," *Chem. Eng. Prog.*, **74**, 70 (1978).
Umeda, T., and T. Kuriyama, "A Logical Structure for Process Control System Synthesis," Proceed. of IFAC Congress, Helsinki, Finland (1978).
Umeda, T., K. Niida and K. Shiroko, "A Thermodynamic Approach to Heat Integration in Distillation Systems," *AIChE J.*, **25**, 423 (1979).
Umeda, T., A. Shindo and A. Ichikawa, "Process Synthesis by Task Assignment," *Chemical Engineering Science*, **29**, p. 2033 (1974).
Wells, G. L., and M. G. Hodgkinson, "The Heat Content Diagram Way to a Heat Exchanger Network," *Process Eng.*, **59**, (1977).
Westerberg, A. W., "A Review of Process Synthesis," to appear ACS Symposium.
Westerberg, A. W., and G. Stephanopoulos, "Studies in Process Synthesis—I. Branch and Bound Strategy with List Techniques for the Synthesis of Separation Schemes," *Chem. Eng. Sci.*, **30**, 963 (1975).
Westerberg, A. W., H. P. Hutchison, R. L. Motard and P. Winter, *Process Flowsheeting*, Cambridge Univ. Press, Cambridge, England (1979).

Manuscript received April 7, 1980; revision received February 2, and accepted February 6, 1981.

Forces on Immersed Tubes in Fluidized Beds

T. C. KENNEDY
J. E. DONOVAN
ATHANASIOS TRIGAS
Department of Mechanical Engineering
Oregon State University
Corvallis, Oregon 97331

The external forces imparted by the bed material on tubes in a fluidized bed contribute to failure of the tubes and their support systems. The objective of this investigation was to provide data on tube forces to be used in structural design. Forces on tubes of various lengths were measured in fluidized beds operating at room temperature. The parameters varied in the experiments were superficial gas velocity and tube array height above the gas distributor. The force-time histories consisted of a series of pulses, whose magnitudes were approximately linearly proportional to tube length. Spectral analyses of the time series indicated that the primary frequency composition of the load was below 25 Hz.

SCOPE

In a variety of technological circumstances, it is necessary to immerse objects in a fluidized bed. In the case of a fluidized bed combustor, the immersed heat exchange tubes are subjected to random loading. The external forces imparted by the bed material on the heat exchange tubes contribute to failure of the tubes and supports. To have a basis for structural design, a definition of the load environment is required. Information on the magnitude and frequency composition of the applied forces is necessary in order to predict the fatigue life of a structure. Data pertinent to the structural design of tubes in a fluidized bed is very limited (Nguyen and Grace, 1978).

The objective of this investigation was to provide data on tube forces to be used in the design of tubes and their support systems in a fluidized bed with primary application toward heat exchange tubes in a combustor facility. Forces on tubes of various lengths were measured over a range of fluidization conditions. Three cold (310°K), fluidized bed facilities were used in the tests. The three beds had the following cross-sectional dimensions: 0.30 m by 0.30 m (1 ft by 1 ft), 0.91 m by 0.91 m (3 ft by 3 ft), and 2.4 m by 0.30 m (8 ft by 1 ft).

Two different types of load cell mechanisms, specifically designed for this application, were used to measure the forces on tubes in these beds. Forces on 5-cm (2-in.) diameter tubes horizontally aligned with lengths of 25, 71, or 244 cm (10, 28 or 96 in.) were measured. The parameters varied in the experiments were superficial gas velocity [1.5, 2.1, 2.7, and 3.3 m/s (5, 7, 9 and 11 ft/s)] and tube array height [25 and 51 cm (10 and 20 in.)] above the gas distributor.

Correspondence concerning this paper should be directed to T. C. Kennedy.

CONCLUSIONS AND SIGNIFICANCE

It was observed in the experiments that the severity of the loading on individual tubes varied with the position of the tube in the array. The bottom tubes were usually the most severely loaded, and the load severity diminished with increasing tube height until it became negligible on the top tubes in the array. The force-time history of the vertical component of the force on the most severely loaded 71 cm (28 in.) long tube consisted of a series of pulses occurring at a rate of 2-3 per second with peak magnitudes of 200-400 N (50-90 lb) and durations of 0.2-0.3 s.

Since the force pulses follow periods during which the force on the tube is negligible, it appears that the force is the result of a front of solids impacting against the tube immediately after the passage of a bubble. A power spectral density analysis of the time series indicated that the primary frequency composition of the load is in the 0-25 Hz range with the peak between 2 and 3 Hz. Measurement of forces on different-length tubes generally indicated that the character of the forces was the same, but that the magnitudes of the pulses were approximately linearly proportional to length. The horizontal component of the force on the tube oscillated from side to side in pulses with magnitudes less than half of those of the vertical force.

The total force on an eight-tube bank representing a continuous serpentine, horizontally aligned run of heat exchange tubing was also measured on the 71 cm (28 in.) long tubes. The vertical force pulses occur here with magnitudes of 550-780 N (125-175 lb) once or twice per second with durations of 0.5-0.8 s. The spectral analysis indicated that the frequency content of the force was very low with a peak between 1 and 2 Hz. The horizontal force-time history was less regular, with force pulses ranging between −90 and 270 N(−20 and +60 lb); but the frequency composition was similar to the vertical force case.

Applying the force data gathered in this investigation to the fatigue design of heat exchange tubes and their support systems is itself a difficult task. Fatigue under random loading is an area of current research, and a universally accepted standard design procedure does not exist at this time. Recently developed approaches require a large calculational effort for a structure as complex as a heat exchange tube array. For preliminary design, a simplified procedure is needed. Fortunately, the nature of the loading on the tube might lend itself to some simple assumptions that make a simplified design procedure possible.

The hostile environment in a fluidized-bed combustor poses many problems in the structural design of heat exchange tubes and their support systems. A number of factors combine to limit the lifetime of the tubes. Erosion of the tube material itself may be augmented by chemical attack or corrosion caused by gas-phase constituents in the fluidized bed. In order to study this effect, it is necessary to conduct tests in which various tube materials under consideration are subjected to the actual environment of a fluidized-bed combustor. The external forces imparted by the bed material on the heat exchange tubes will also contribute to failures not only of the tubes, but possibly of the support system that holds them in place. Unlike corrosion, the forces on heat exchange tubes can be studied in a cold, fluidized bed, and the results can be used in the design of a hot bed.

A structural design basis requires a definition of the load environment. Information on the magnitude and frequency composition of the applied forces is necessary in order to predict the fatigue life of a structure (Buxbaum, 1979). The immersed heat exchange tubes in a fluidized-bed combustor are subjected to random loading. The forces on the tubes include the effect of buoyancy (the bed material behaves like a liquid), form drag related to the rate of change of momentum as the solids flow around the tube, and some viscous drag related to the velocity of particles passing the tube.

In this investigation, experiments were performed to provide data on tube forces to be used in the design of heat exchange tubes and support systems in a fluidized-bed combustor. Forces on simulated heat exchange tubes of various lengths were measured over a range of fluidization conditions. The parameters varied in experiments conducted in cold (310°K), fluidized beds were tube length, superficial gas velocity and tube array height above the distributor plate.

FACILITIES

Three fluidized-bed facilities were used in the tests. These beds had the following cross-sectional dimensions: 0.30 × 0.30 m (1 × 1 ft), 0.91 × 0.91 m (3 × 3 ft), and 2.4 × 0.30 m (8 × 1 ft). Two different types of load cell mechanisms were used to measure the forces on 5 cm (2 in.) diameter tubes aligned horizontally in these beds. A description of the test facilities, instrumentation, and data collection system is given below.

Test Facilities

The 1 × 1 fluidized bed has a cross section of 0.30 × 0.30 m (1 × 1 ft) and a test section height of 0.6 m (2 ft). Fluidizing air is supplied by a rotary, positive displacement blower with a maximum capacity of 3.78 m^3/s at 51.7 KPa (8000 cfm at 7.5 psi). The air from the blower enters a plenum below the air distributor which consists of a perforated plate. The air flow is monitored with a venturi meter, and the superficial gas velocity is controlled by the speed of the blower. This bed accepts an array of 25 cm (10 in.) long tubes.

The 3 × 3 fluidized bed has a cross section of 0.91 m by 0.91 m (3 ft by 3 ft) and a test section height of 1.4 m (4.5 ft). This bed is powered by the same blower and operates with much of the same duct work as the 1 × 1 bed. A series of valves is used to channel air through the appropriate passages. This bed accepts an array of 71 cm (28 in.) long tubes.

The 8 × 1 fluidized bed has a cross section of 2.4 m by 0.30 m (8 ft by 1 ft) and a test section height of 1.2 m (4 ft). It also operates with the same blower and much of the same duct work as the 1 × 1 bed and accepts an array of 240 cm (96 in.) long tubes.

Instrumentation

Forces on individual tubes in the 1 × 1 and 3 × 3 beds were measured by supporting each end of a 5 cm (2 in.) diameter tube with strain gage load cells that were designed and built for this specific application (Kennedy, 1980). These load cells have the capability of measuring both the vertical and horizontal (normal to the tube axis) components of force transmitted by the tube to its end supports. The load cells were calibrated by applying known static loads to the tubes and relating the voltage output from the strain gage bridge circuit to the magnitude of the load.

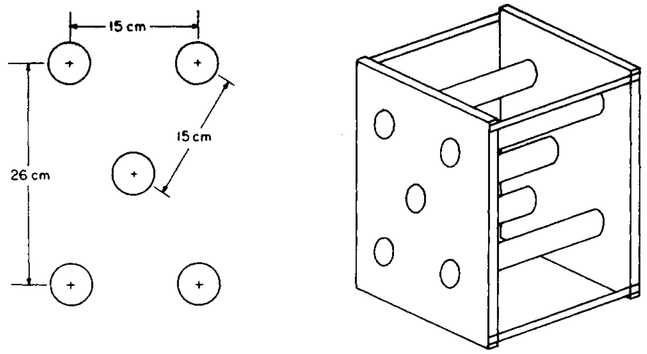

Figure 1. Tube array in 1 × 1 bed.

This calibration is also valid for dynamic loads, provided that the frequency components in the load-time history are considerably less than the natural frequency of the load cell—heat-exchange tube system.

The natural frequency was found in a shake table test to be about 150 Hz for the 71 cm (28 in.) long tube used in the 3 × 3 bed. It should be substantially higher for the 25 cm (10 in.) long tube used in the 1 × 1 bed. Forces were measured on individual tubes forming part of an array. In the 1 × 1 bed the center tube in a five-tube array was instrumented as shown in Figure 1. This array was bolted to the walls of the bed during testing. In the 3 × 3 bed, an eight-tube bank in the center of a larger array was instrumented as shown in Figure 2.

In the 8 × 1 bed, one tube at the center of an array of eleven 244 cm (96 in.) long tubes was instrumented for force measurement. The 244 cm (96 in.) length of the tube required that it be supported by load cells at four points along its length to insure a high enough natural frequency so that force-time histories could be obtained without significant distortion. Details on the design of the load cells are given in Kennedy (1980). Again the load cells were calibrated statically by placing a known weight on the cell and measuring the output. This calibration is valid for dynamic loads provided that the natural frequency of the system is sufficiently high. In this case, the natural frequency was calculated from a finite element analysis, which included the apparent mass (Fung, 1969) of the bed material, using the SAP IV program (Bathe et al., 1974). The lowest natural frequency of the system was found to be 107 Hz which was considered to be high enough to insure minimum signal distortion.

Data Collection and Analysis

The signals from all the load cells were fed into amplifier cards which were located in an electrical console outside the beds. The console was wired to a minicomputer, in which machine language programs were used to collect data at specified sampling rates and time intervals. The digitized data were stored initially on a disk and was later transferred to a magnetic tape for processing on a large digital computer.

In most instances, tube force data are presented in the form of a short (5-s duration) force-time history and a power spectral density PSD vs. frequency plot for the time series. The program used in the PSD analysis was FTFFT1 from the IMSL library which used a Parzen spectral window and averages spectral estimates made from short segments of the entire time series (Welch, 1967). In this investigation, the analysis was made from records 25 to 40 s in duration at sampling rates of 250 to 310 samples per second. Each record was broken into 15 to 20 segments for averaging.

TEST RESULTS

Forces on 5 cm (2 in.) diameter tubes with lengths of 25, 71, or 244 cm (10, 28 or 96 in.) in arrays with a tube spacing of 15 cm (6 in.) between centers were measured at superficial gas velocities of 1.5, 2.1, 2.7 and 3.3 m/s (5, 7, 9, and 11 ft/s). E116 sand with a

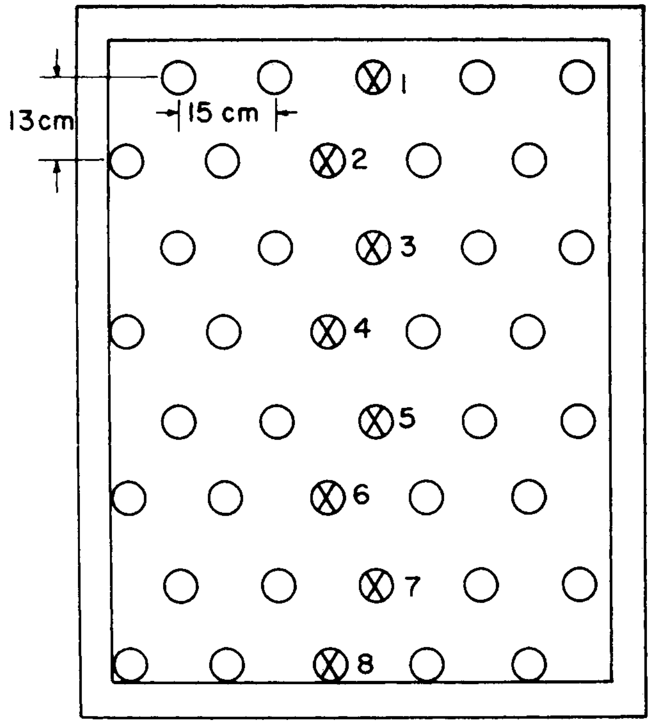

Figure 2. Locations of instrumented tubes in 3 × 3 bed.

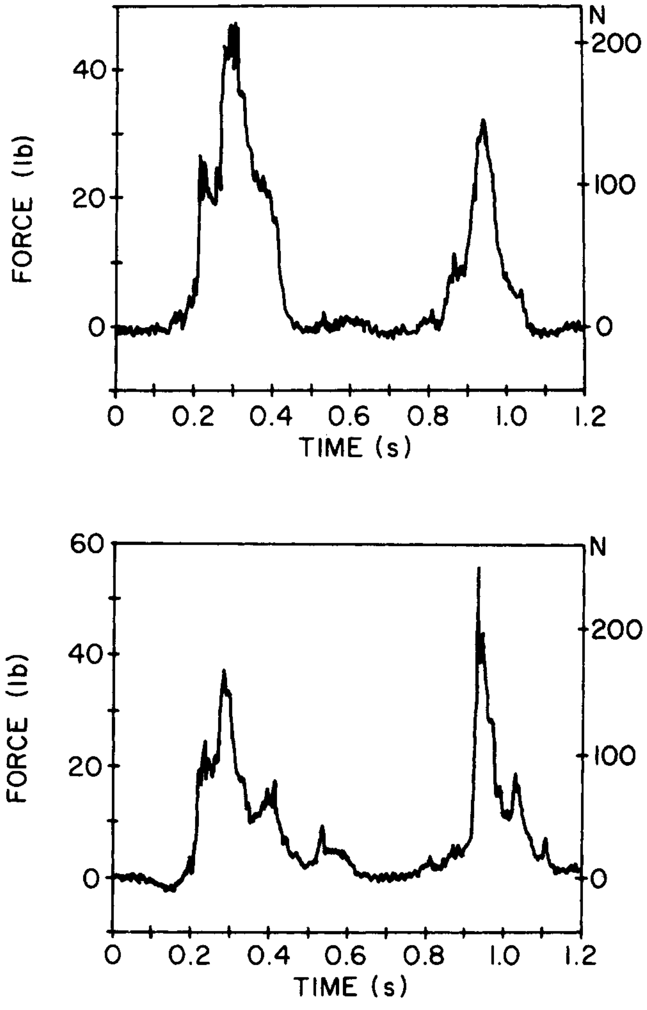

Figure 3. Vertical forces at opposite ends of a 71 cm long tube.

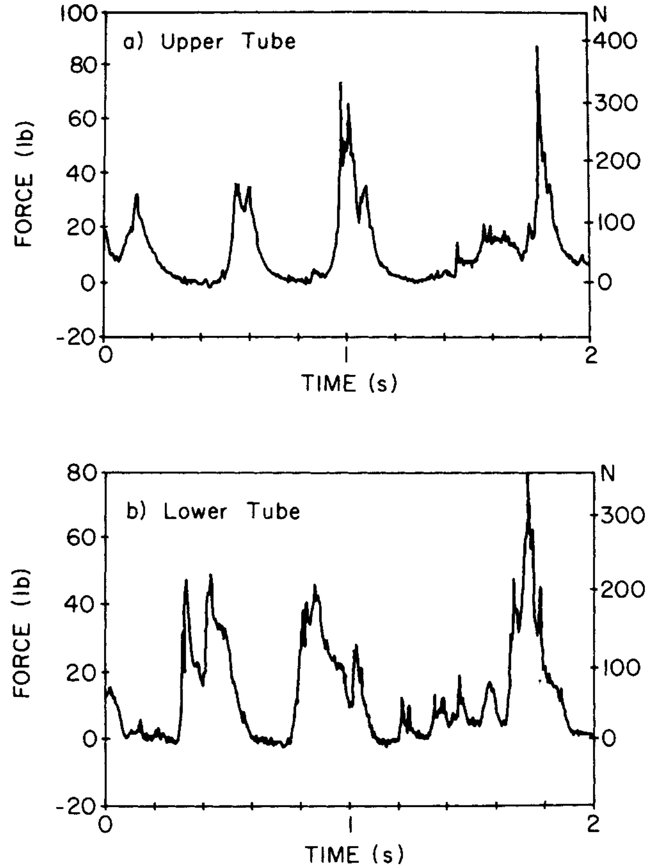

Figure 4. Vertical forces on adjacent 71 cm long tubes.

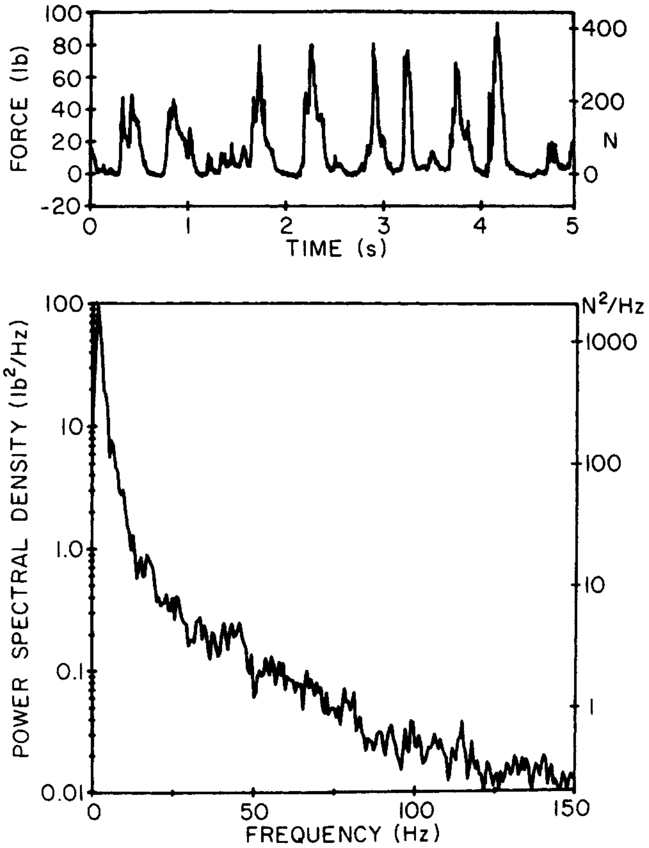

Figure 5. Vertical forces on a single 71 cm long tube with 51 cm array height.

mean particle diameter of 0.8 mm (0.03 in.) and a density of 2700 kg/m^3 (167 lb/ft^3) was used as the bed material. The depth of the bed was 56 cm (22 in.) in the 1 × 1 bed and 89 cm (35 in.) in the 3 × 3 and 8 × 1 beds. The minimum fluidization velocity was measured by Colakyan (1979) to be 0.46 m/s (1.5 ft/s). The void fraction of the bed was 0.43 in the defluidized state and 0.5-0.65 during fluidization.

Results in 3 × 3 Bed

The vertical and horizontal (normal to the tube axis) components of the forces transmitted to the supports at the ends of a 71 cm (28 in.) long tube in the 3 × 3 bed were measured. Tests were conducted with the bottom of the array at elevations of 25 and 51 cm (10 and 20 in.) above the distributor plate.

For the 51 cm (20 in.) array elevation, the loading was most severe on those tubes near the bottom of the array. The load severity diminished with increasing tube height, until it became negligible on the top tube. Vertical force data (upward force is positive) from the load cells at the right and left ends of the bottom tube (number 8 in Figure 2) at a superficial gas velocity V = 2.1 m/s (7 ft/s) are shown in Figure 3. The force-time histories consist of pulses with durations of 0.2-0.3 s. Since the pulses follow periods during which the force on the tube is negligible, it appears that the force is the result of a front of solids impacting against the tube immediately after the passage of a bubble. The pulses in the force at each end occur simultaneously, although the magnitudes generally are different. A magnitude larger at one end than the other indicates an uneven distribution of force on the tube, probably caused by the passage of a bubble on one side of the tube.

Force data from two adjacent tubes are given in Figure 4. Figure 4a shows the total vertical force on tube number 6 (upper tube), and Figure 4b shows similar data for tube number 8 (lower tube). Pulses on the lower tube precede those on the tube above it by 0.15 to 0.25 s. The distance between these tubes is 26.4 cm (10.4 in.). Thus, the pulse appears to propagate upward through the array at a velocity of 1-1.7 m/s (3-5 ft/s) which corresponds to the rise velocity of bubbles observed in the bed (Fitzgerald, 1980).

More results of tests at the 51 cm (20 in.) array height are given in Figures 5 through 7 for V = 2.1 m/s (7 ft/s). In Figure 5, the vertical force data from the most severely loaded tube (at the bottom of the array) are given in the form of a short force-time history and a PSD plot. The force appears as pulses occurring at a rate of 2-3 per second with magnitudes typically around 300-450 N (70-100 lb). A spectral analysis of this record given in the PSD plot indicates that the primary frequency composition of the load is in the 0-25 Hz range with the peak between 2 and 3 Hz. This peak corresponds to the rate at which pulses occur in the force-time history.

The horizontal force on this same tube is shown in Figure 6. The force oscillates from side to side and has a mean value very close to zero. Although the frequency content of the horizontal forces is very similar to that of the vertical forces, the magnitudes of the pulses here are less than half those of the vertical forces.

The total vertical force on the eight-tube instrumented array, obtained by summing the vertical force signals from each load cell, is shown in Figure 7. The pulses appear here with magnitudes of 600 to 800 N (140 to 180 lb) once or twice per second with a duration of 0.5 to 0.8 s. The PSD plot indicates that the frequency content of the forces is very low with a peak between 1 and 2 Hz.

The total horizontal force on the eight-tube instrumented array, obtained by summing the horizontal force signals from each load cell, was also measured. Most of the pulses vary between −90 and +270 N (−20 and +60 lb) with a duration of 0.2 to 0.8 s and a frequency of 1-2 Hz. Again, a PSD plot

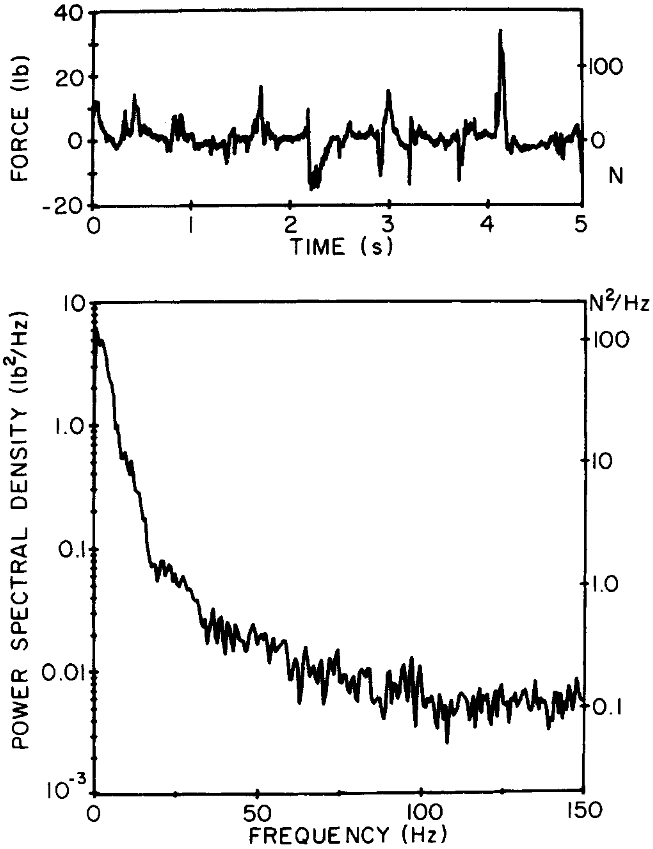

Figure 6. Horizontal forces on a single 71 cm long tube with 51 cm array height.

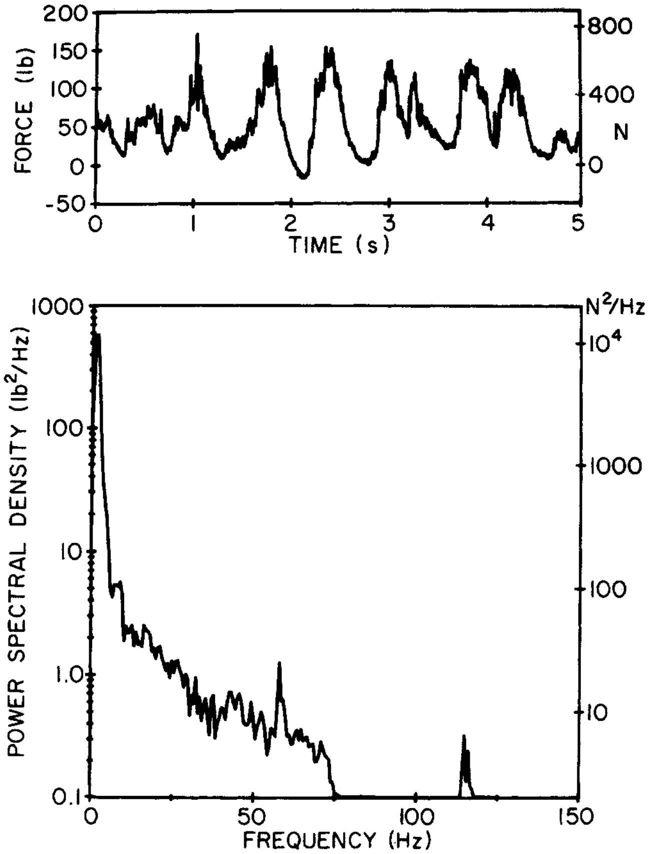

Figure 7. Total vertical forces on an eight-tube array of 71 cm long tubes with 51 cm array height.

indicates that the low frequencies dominate. The data for other superficial gas velocities in this set of tests were very similar to that just shown, with moderate differences in the amplitude of the forces. The effect of superficial gas velocity is discussed later.

The experiments just described were repeated with the bottom of the array lowered to a height of 25 cm (10 in.) above the distributor. In this case, the loading was found to be most severe on those tubes near the center of the array. The magnitudes of the pulses on the tubes at the bottom of the array were about half those on tubes near the center. For tubes near the top of the array, the loading was even less severe. In Figure 8, the vertical force data from the most severely loaded tube, in this case tube number 5, are given. There is a great deal of similarity between this data and that shown earlier for the 51 cm (20 in.) array height. The force appears as pulses occurring at a rate of 2-3 per second, and the primary frequency composition is in the 0-25 Hz range. However, the magnitudes of the pulses are typically 90-180 N (20-40 lb), about half those for the 51 cm (20 in.) array height. This result is expected because the higher array height permits the gas bubbles to grow to a larger size before they are broken up as they pass through the tube array. The larger bubbles have the ability to transfer more momentum to the tubes than do the smaller ones, thus producing larger forces.

The root-mean square (RMS) vertical forces, which are measures of the intensity of the forces, are plotted against superficial gas velocity in Figure 9. The vertical forces appear to level off or even decrease in intensity at high gas velocities. Similar behavior was observed for the horizontal forces.

Results of Tests in 1 × 1 and 8 × 1 Beds

Force measurements were made on tubes in the center of arrays which were approximately 25 cm (10 in.) above the distributors in the 1 × 1 and 8 × 1 beds. Tests were conducted at superficial gas velocities of 1.5, 2.1 and 2.7 m/s (5, 7 and 9 ft/s). A force-time history of the vertical force on a 25 cm (10 in.) long tube in the 1 × 1 bed is shown in Figure 10 for V = 2.1 m/s (7

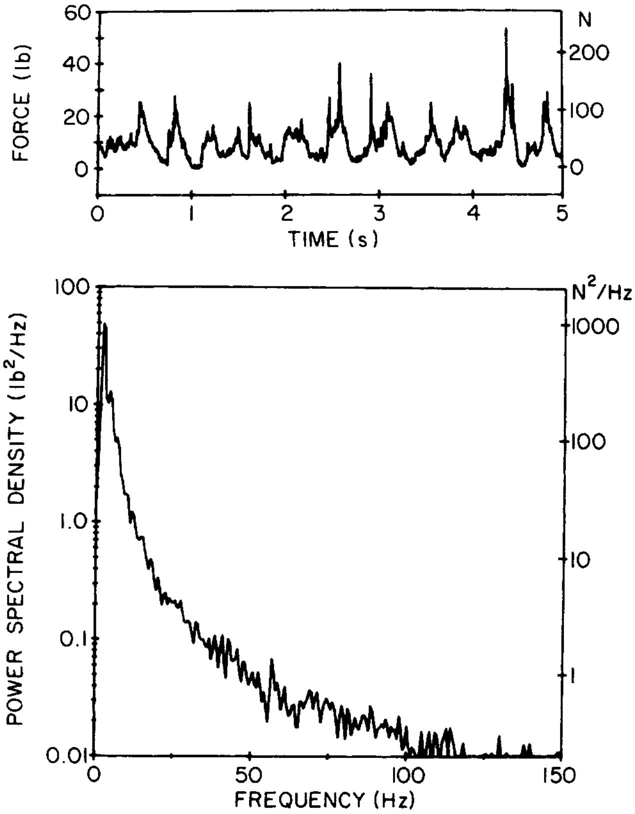

Figure 8. Vertical forces on a single 71 cm long tube with 25 cm array height.

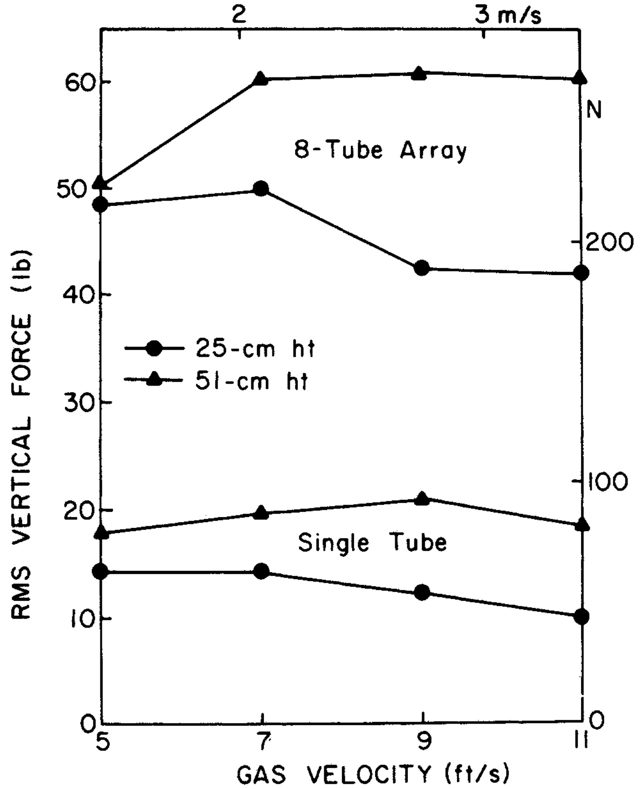

Figure 9. RMS vertical force vs. air velocity for 71 cm long tubes.

ft/s). This force-time history consists of pulses, typically on the order of 44-67 N (10-15 lb), that have durations of 0.1-0.2 s and occur at a rate of 2-3 times per second. This is similar to the data shown in Figure 8 for the 71 cm (28 in.) long tube except that the magnitudes of the pulses are about a factor of two lower here.

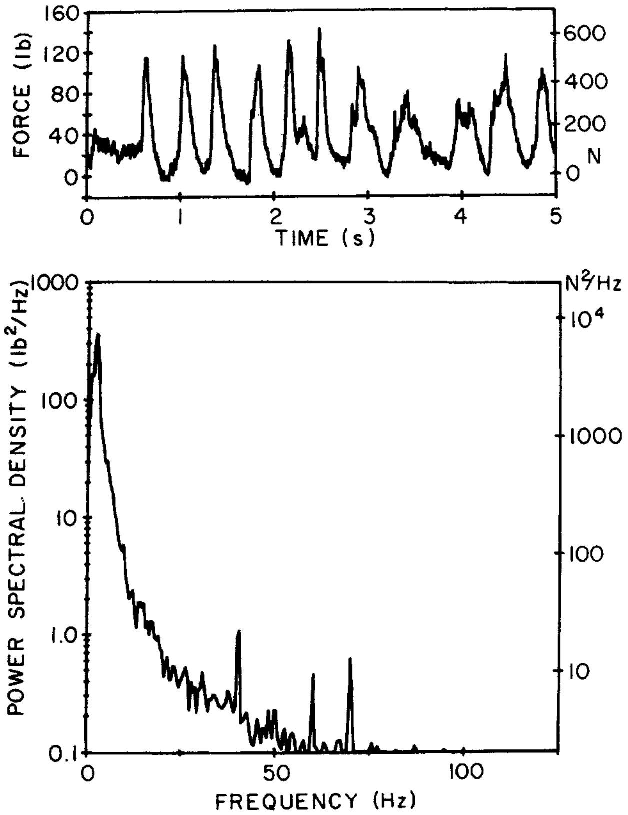

Figure 11. Vertical forces on a single 244 cm long tube with 25 cm array height.

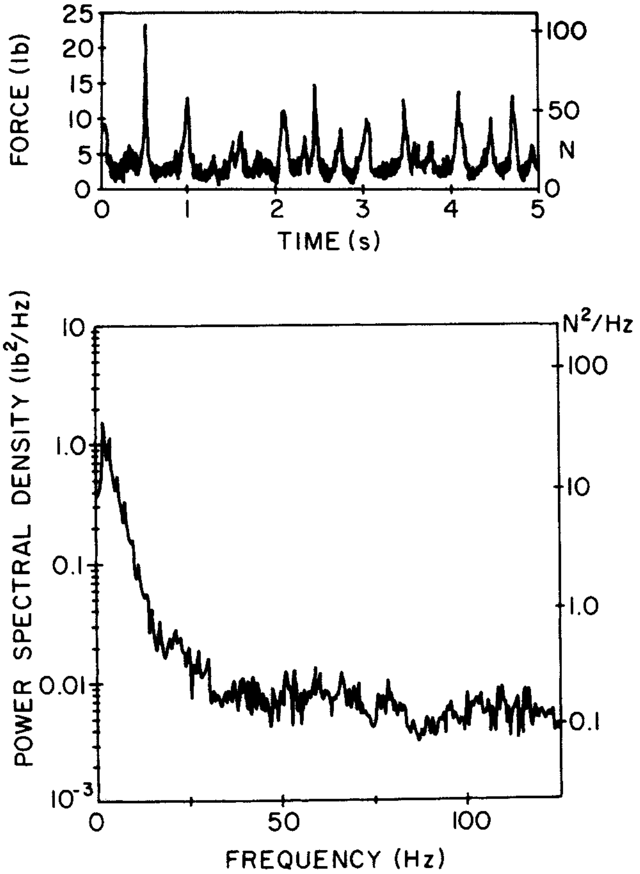

Figure 10. Vertical forces on a single 25 cm long tube with 25 cm array height.

The PSD plot for this record indicates that the primary frequency composition of the load is in the 0-25 Hz range with the peak between 2 and 3 Hz as was the previous case. Data taken at superficial gas velocities of 1.5 and 2.7 m/s (5 and 9 ft/s) were very similar to that shown in Figure 10.

In the 8 × 1 bed, the vertical components of the force transmitted to the supports at four points along the length of a 244 cm (96 in.) long tube were measured for $V = 1.5, 2.1$, and 2.7 m/s (5, 7, and 9 ft/s). The total vertical force on the tube, obtained by summing the output from the four load cells, is shown in Figure 11 for $V = 2.1$ m/s. The character of the data is very similar to that observed in the smaller beds. Force pulses appear at a rate of 2-3 per second, and the primary frequency content is below 25 Hz. The magnitudes of the force pulses are quite high with many peaks in excess of 445 N (100 lb). Additional, more detailed force data may be found in Kennedy (1980).

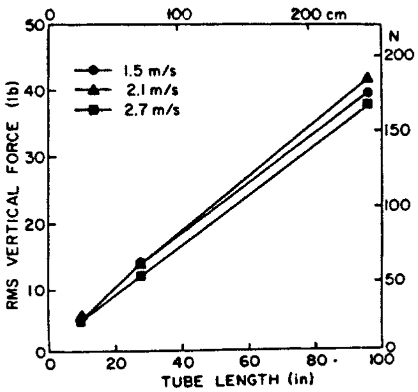

Figure 12. RMS vertical force vs. tube length for a single tube.

Effect of Tube Length

Fluidized-bed combustor facilities presently envisioned are considerably larger than the ones used in tests in this investigation. It would be desirable to be able to extrapolate the data presented here to any length of tube. Consolidation of the data from tests on 25, 71 and 244 cm (10, 28 and 96 in.) long tubes in a plot of RMS vertical force vs. tube length for various superficial gas velocities is shown in Figure 12. As would be expected, the slopes of the curves decrease with increasing tube length. However, this decrease is slight. Extrapolating the curves to longer tube lengths as straight lines would probably result in a slight overestimation of the RMS force. If the magnitudes of the pulses in the forces for various tube lengths are compared, approximately the same dependence on length as the RMS force is observed.

DISCUSSION

Bubble Movement—Tube Force Relationship

The load cell data support the view that the force pulses on the tubes are produced by the passage of bubbles. In addition, several experiments were run with a capacitance probe attached to one of the tubes to detect the presence of bubbles near the tube. The capacitance probe records indicated that the frequency of large bubbles passing the tube was the same as the frequency of pulses in the force-time history; i.e., about 2-3 per second. As was discussed earlier in reference to Figure 4, the disturbance producing the force pulse appears to travel upward through the array at a velocity of 1-1.7 m/s (3-5 ft/s) which corresponds to the velocity of large bubbles observed in the bed. Thus, the observed frequency and velocity of the bubbles are consistent with the load cell data.

While it is clear that the force pulses are related to bubble movement, a description of the mechanism which produces the force pulses and the development of an analytical model to quantitatively predict the forces is a difficult undertaking. The behavior of bubbles in fluidized beds of intermediate and large-size particles with immersed tubes is an area of current research (Lowe et al., 1979; Fitzgerald, 1980) and is not well understood for various regimes of fluidization.

It appears that the forces on the tubes are the result of an impulse caused by the transfer of the momentum of a body of solids in the wake of a bubble striking the tube. Presently, there is insufficient knowledge of bubble mechanics for the types of fluidized beds considered here to predict both the mass and velocity of the body of solids whose momentum is transferred to the tubes.

Design Considerations

Applying the force data gathered in this investigation to the fatigue design of heat exchange tubes and their support systems is a nontrivial task. Fatigue under random loading is an area of current research, and a universally accepted standard design procedure does not exist at this time. There are two approaches to this problem. One is a modification of the traditional S-N fatigue curve analysis in which deterministic or random fatigue data is used in a damage law (Wirsching and Haugen, 1974). The other is a more phenomenological approach in which crack growth models are used (Wei, 1978; Barsom, 1976). Both of these approaches require an enormous calculational effort for a structure as complex as a heat exchange tube array (Petyt, 1975; Kennedy, 1980).

For preliminary design a simplified procedure is needed. Fortunately, the nature of the loading on the tube might lend itself to some simplifying assumptions that make a simplified preliminary design procedure possible. The random force-time history in Figure 7, which represents the total loads on a continuous serpentine, horizontally aligned run of heat exchange tubing, may be approximated by deterministic, sinusoidally-varying forces with a frequency of 1.5 Hz (Kennedy, 1980). Because the frequency of the forcing functions is so low, they may be assumed to be essentially quasistatic in nature so that a static stress analysis of the structure is all that is required. The prediction of the fatigue life of a structure under these conditions is straightforward (Juvinal, 1973) and should lead to a conservative design.

Future Work

Clearly this investigation has the limitation that the experiments were conducted in cold, fluidized beds which only approximate the conditions in a hot bed. A very limited number of experiments have been performed in a high-temperature bed (Khan, 1979; Kennedy, 1980). Although these experiments generally indicated that there were no significant differences in the character of the tube forces at high temperature compared to those at low temperature, further testing is required before definite conclusions can be reached.

The data presented here appears to indicate a strong relationship between bubble movement and tube forces. As discussed earlier, it seems reasonable to assume that the force is the result of a front of solids impacting against the tube immediately after the passage of a bubble. This explanation requires verification that could be obtained by experiments in a two-dimensional bed in which cine-photography is used in conjunction with load cell measurements.

ACKNOWLEDGMENT

This research was supported by the Electric Power Research Institute and Babcock & Wilcox Co. on Project Number RP718-2. The authors are indebted to T. J. Fitzgerald of Oregon State University for many helpful suggestions during the course of this research.

NOTATION

V = superficial gas velocity

LITERATURE CITED

Barsom, J. M., "Fatigue Crack Growth Under Variable-Amplitude Loading in Various Bridge Steels," *ASTM STP 595*, 217 (1976).

Bathe, K. J., E. L. Wilson, and F. E. Peterson, "SAP IV—A Structural Analysis Program for Static and Dynamic Response of Linear Systems," Rept. No. EERC 73-11, UC, Berkeley (1974).

Buxbaum, O., "Random Load Analysis as a Link Between Operational Stress Measurement and Fatigue Life Assessment," *ASTM STP 671*, 5 (1979).

Colakyan, M., "Elutriation From Fluidized Beds With and Without Immersed Tubes," M.S. Thesis, Oreg. St. Univ. (1979).

Fitzgerald, T. J., "Investigation of Fluidized Beds with Immersed Heat Exchange Tubes," EPRI Report, CS-1476 (1980).

Fung, Y. C., *The Theory of Aeroelasticity*, Dover Pub., 69 (1969).

Juvinall, R. C., *Stress, Strain, and Strength*, McGraw-Hill, 268 (1967).

Khan, W. M., "A System for Measuring Forces on Immersed Tubes in a Hot Fluidized Bed," M.S. Project Rept., Oreg. St. Univ. (1979).

Kennedy, T. C., "A Study of Forces on Immersed Tubes in Fluidized Beds," EPRI Report, CS-1542 (1980).

Lowe, O., B. Shmutter, and W. Resnick, "Particle and Bubble Behavior and Velocities in a Large-Particle Fluidized Bed with Immersed Obstacles," *Powder Tech.*, **22**, 45 (1979).

Nguyen, T. H., and J. R. Grace, "Forces on Objects Immersed in Fluidized Beds," *Powder Tech.*, **19**, 255 (1978).

Petyt, M., "Finite Element Methods for the Response of Structures to Random Excitations," World Cong. Finite Element Meth. in Struct. Mech., 16.1 (1975).

Wei, R. P., "Fracture Mechanics Approach to Fatigue Analysis in Design," *J. Eng. Mat. Tech.*, **100**, 113 (1978).

Welch, P. D., "The Use of Fast Fourier Transform for the Estimation of Power Spectra: A Method Based on Time Averaging Over Short, Modified Periodograms," *IEEE Trans.*, **AV-15**, 70 (1967).

Wirsching, P. H., and E. B. Haugen, "A General Statistical Model for Random Fatigue," *J. Eng. Mat. Tech.*, **96**, 34 (1974).

Manuscript received October 30, 1979; revision received July 28, and accepted July 31, 1980.